Algal Research 91 (2025) 104187

Contents lists available at ScienceDirect

Algal Research

journal homepage: www.elsevier.com/locate/algal

# The stress response strategies of two typical coral Symbiodiniaceae (*Cladocopium goreaui* and *Durusdinium trenchii*) under abnormal temperatures

Jiayuan Liang [a,*,1], Liangyun Qin [a,1], Li Zhang [c,1], Yongqian Xu [a], Tianyi Niu [a], Zhicong Li [a], Yating Yang [a], Zhuqing Liang [a], Kefu Yu [a,b,*], Sanqiang Gong [d]

[a] *Guangxi Laboratory on the Study of Coral Reefs in the South China Sea, School of Marine Sciences, Guangxi University, Nanning 530004, China*
[b] *Southern Marine Science and Engineering Guangdong Laboratory (Guangzhou), Guangzhou 510030, China*
[c] *School of Resources, Environment and Materials, Guangxi University, Nanning 530004, China*
[d] *Key Laboratory of Tropical Marine Bio-resources and Ecology & Guangdong Provincial Key Laboratory of Applied Marine Biology, South China Sea Institute of Oceanology, Chinese Academy of Sciences, Guangzhou 510301, China*

ARTICLE INFO

*Keywords:*
Coral reefs
Symbiodiniaceae
Environmental adaptability
Global change
South China Sea

ABSTRACT

Temperature stress disrupts the coral–Symbiodiniaceae symbiosis and contributes to coral bleaching. Symbiodiniaceae, essential symbionts for reef-building corals, provide over 90 % of the coral holobionts photosynthetic energy. This study examined the thermal response strategies of two Symbiodiniaceae types, *Cladocopium goreaui* (*C. goreaui*) and *Durusdinium trenchii* (*D. trenchii*), at high (34 °C) and low (16 °C) temperatures. *C. goreaui* exhibited heat sensitivity, with reduced cell density, impaired photochemical efficiency of photosystem II (PSII) (*Fv/Fm*), pigment loss, and chloroplast degradation. In contrast, *D. trenchii* maintained photosynthetic performance and upregulated proteins related to heat shock response, antioxidant defense, and membrane stability. Under cold stress, both species showed moderate physiological changes. *C. goreaui* activated pathways associated with redox homeostasis and the TCA cycle, indicating enhanced cold tolerance. *D. trenchii* primarily responded by upregulating RNA splicing-related pathways, suggesting an adaptive post-transcriptional regulation mechanism. These results highlight distinct thermal response strategies and provide insight into species-specific resilience among Symbiodiniaceae under climate stress.

## 1. Introduction

The cornerstone of coral reef ecosystems is the "holobiont" composed of coral polyps and their associated microorganisms, which include Symbiodiniaceae, bacteria, fungi, and protists. Among these, Symbiodiniaceae contribute >95 % of the photosynthetic products (e.g., amino acids, glucose, glycerol) to the "holobiont" [1,2]. Simultaneously, they acquire the essential carbon dioxide and nutrients (such as ammonia and phosphate) necessary for their survival and for photosynthesis from the coral host [3]. The stable symbiosis between coral hosts and Symbiodiniaceae is crucial for the health of coral reef ecosystems [4]. When the surrounding environment undergoes abnormal changes, the stability of the "holobiont" is compromised, leading to coral bleaching and, ultimately, death. Among the various stresses, abnormal seawater temperature is a primary factor affecting the stability of the "holobiont". However, extensive field survey data indicate that not all coral species undergo bleaching and death in the face of extreme temperature stress. Some species exhibit resilience to high-temperature and survive under such conditions [5,6]. These temperature resistance characteristics are closely related to both the coral host and the specific Symbiodiniaceae species involved [7–11].

LaJeunesse et al. [12] proposed that the Symbiodiniaceae clades actually represent up to 15 distinct species in morphologically or phylogenetically. Physiological characteristics and environmental tolerances vary significantly among different species of Symbiodiniaceae, aiding coral hosts in resisting external environmental stressors. Recent research generally suggests that some species within the genus *Durusdinium* (clade D), such as *D. trenchii* in the D1and D1a/D1–4 clades, are

* Corresponding authors.
*E-mail addresses:* jyliang@gxu.edu.cn (J. Liang), kefuyu@scsio.ac.cn (K. Yu).
[1] These authors contributed to the work equally and should be regarded as co-first authors.

https://doi.org/10.1016/j.algal.2025.104187
Received 16 January 2025; Received in revised form 15 June 2025; Accepted 2 July 2025
Available online 17 July 2025

evolved to thrive in extremely high temperatures and high-turbidity environments [13]. When establishing symbiotic relationships with cnidarians (corals and anemones), these species can resist the breakdown of the symbiotic system induced by stress from abnormal environmental conditions, known as coral bleaching [14]. Research by Manzello et al. [15] demonstrated that *D. trenchii* improves the thermal resilience of the coral *Orbicella faveolata*, enabling this species to persist through extensive thermal bleaching episodes in the Florida Keys. *Durusdinium* are widely distributed in the Indo-Pacific and are also found in coral reefs in the South China Sea at mid to low latitudes [16]. On the other hand, *Cladocopium* (clade C) is one of the most diverse genera of Symbiodiniaceae, with different subclades exhibiting distinct physiological characteristics. Subclade C1 contains several species that form symbiotic relationships with corals in the Indo-Pacific region, often displaying high photochemical efficiency of PSII (*Fv/Fm*) and helping coral hosts tolerate seasonally low temperatures and high-nutrient conditions [17]. Species within the C15 subclade mainly form stable symbiotic relationships with corals in the genus *Porites*, which tolerate high temperatures and turbidity [18].

In various coral reef regions in the South China Sea at different latitudes, including the Nansha Islands, Xisha Islands, Luhuitou in Sanya, Leizhou Peninsula, Weizhou Island, Daya Bay, and Dongshan Island, the dominant Symbiodiniaceae genera associated with reef-building corals are *Cladocopium* (Clade C) and *Durusdinium* (Clade D) [16]. At the subclade level, there are significant differences in the composition of Symbiodiniaceae communities among coral species in coral reef regions at different latitudes [19]. Specifically, in relatively high-latitude reef-building corals in the South China Sea, the Symbiodiniaceae community is predominantly composed of the C1 subclade [20]. In contrast, in mid- to low-latitude reef-building corals, the Symbiodiniaceae community is dominated by diverse subclade types, including the C50, Cspc, C15, C1, and D1 subclades [18,20,21]. Overall, the community composition of Symbiodiniaceae in South China Sea corals shows a spatial distribution pattern transitioning from the dominance of the C1 subclade at higher latitudes to the codominance of heat-tolerant Symbiodiniaceae such as C15, C3u, and D1 at mid- to low latitudes [16].

The evidence above indicates that the unique identity of Symbiodiniaceae influences the adaptability of corals to their environment [22]. However, the specific biological functions of different species of Symbiodiniaceae, especially their response strategies under temperature changes, have not been fully elucidated. Due to the unique symbiotic relationship between Symbiodiniaceae and corals, very few species can be cultured outside their host organisms for an extended period. Ahles et al. [23] conducted in vitro cultivation studies on Symbiodiniaceae from 70 different hosts and reported that <25 % could survive briefly in ASP-8A medium. Using f/2 medium, Kinzie [24] also reported that only a few species of Symbiodiniaceae survived in vitro cultivation. Additionally, K medium [24] and ISM medium [25] have been applied for in vitro cultivation of Symbiodiniaceae but with suboptimal results.

In the preliminary stages of our research, two Symbiodiniaceae strains, were isolated and cultured: a *Cladocopium* species (C1 type) from *Acropora pruinosa* in the relatively high-latitude coral reef areas of Weizhou Island; and a *Durusdinium* species (D1 type) from *Galaxea fascicularis* in the low-latitude coral reef area of the Xisha Islands in the South China Sea [26]. This study focused on these species, aiming to explore their response strategies under abnormal temperatures of 34 °C and 16 °C. The goal of this study was to gain a deeper understanding of the mechanisms of environmental adaptation in coral reefs and future evolutionary trends from the perspective of these key symbiotic partners.

## 2. Materials and methods

### 2.1. Cultivation of and experimental design for C. goreaui and D. trenchii

The Symbiodiniaceae strains used in this study were isolated and cultured from coral reefs in the South China Sea in the preliminary phase of the project. The species were identified as *Cladocopium goreaui* (*C. goreaui*) (100 %) and *Durusdinium trenchii* (*D. trenchii*) (100 %) through ITS and LSU sequence determination and homology search [26], respectively. Prior to the experiments, Symbiodiniaceae strains were cultured in L1 medium at 25 °C under a light intensity of 90 μmol photons $m^{-2}$ $s^{-1}$, the Symbiodiniaceae were cultivated to the mid-logarithmic phase to ensure optimal growth conditions. For the temperature stress experiments, mid-logarithmic *C. goreaui* and *D. trenchii* cultures were centrifuged at 800 ×*g* for 5 min, the supernatant was removed, and the cells were transferred to 500 mL conical flasks containing 300 mL of L1 medium. The initial cell concentration was adjusted to $1.0 \times 10^5$ cells/mL, and the cultures were maintained for 1 day before the temperature stress experiment was initiated. The lowest monthly mean sea surface temperature (SST) was 17.3 °C between 1960 and 2001 [27]. SST below 18 °C in winter was found to severely affect corals [28]. By analysing satellite SST data from 1985 to 2019 (https://coralreefwatch.noaa.gov), we found that the SST at Weizhou Island is generally around 30 °C in summer and 19 °C in winter. The SST around Weizhou Island has been increasing at a rate of 0.33 °C/10 yr over the past decades [27]. Different temperature conditions were used, including a normal cultivation temperature of 25 °C (control group), an abnormally high temperature of 34 °C (to simulate possible future seawater temperatures [29]), and an abnormally low temperature of 16 °C (to simulate seawater temperatures under extreme cold conditions in winter). On day 0, cultures of both *C. goreaui* and *D. trenchii* were transferred into conical flasks. For the high- and low-temperature groups, the temperature was adjusted from 25 °C by increasing or decreasing 1 °C every 8 h until the target temperature was reached, followed by a 10-day temperature stress period. Each group included three biological replicates. Measurements of cell density, *Fv/Fm*, and chlorophyll content were conducted at 12:00 PM on days 1, 4, 7, 10, and 14.

### 2.2. Cell density and growth rate determination

A 1 mL aliquot of algal culture was fixed by adding 100 μL of formaldehyde reagent. Cell counting for Symbiodiniaceae was performed using a plankton counting chamber under an upright optical microscope (Nikon, ECLIPSE Ni-E). The data were recorded, and cell density was calculated. The growth rate (μ) was determined using the formula $\mu = \ln(N2/N1)/(t2\text{-}t1)$, where μ is the growth rate, N2 and N1 are the cell densities at times t2 and t1, respectively, which are calculated by the stress temperature arrival time t1, that is, the initial density under stress conditions on day 4.

### 2.3. Determination of the photochemical efficiency of PSII (Fv/Fm)

The *Fv/Fm* value can indicate the energy conversion efficiency of PSII in photosynthetic organisms. According to the methods of Guo et al. [30], *Fv/Fm* was measured during dark adaptation for 30 min with a Moni-DA Plant Monitoring PAM (WALZ, Germany), the maximum fluorescence value (*Fm*) was determined by a 0.6 s saturation pulse (approximately 8000 μmol $m^{-2}{\cdot}s^{-1}$).

### 2.4. Determination of photosynthetic pigment levels

Ten milliliters of algal culture was centrifuged at 5000 ×*g* for 5 min, after which the supernatant was removed. Then, 1 mL of 100 % methanol solution was added, followed by vortexing and shaking. The mixture was stored in the dark at 4 °C for 24 h. After extraction, the absorbance at 480 nm, 510 nm, 630 nm, 664 nm, and 750 nm was measured using a spectrophotometer (Thermal). The concentrations of chlorophyll *a* (Chl a) and carotenoids (CARs) in the Symbiodiniaceae were calculated using the formulas provided by Ritchie et al. [31].

$$\text{Chlorophyll a}(\mu g/ml) = 13.6849 \times (A_{664} - A_{750}) - 3.4551 \times (A_{630} - A_{750})$$

$$\text{Carotenoids}(\mu g/ml) = 7.6 \times (A_{480} - A_{750}) - 1.49 \times (A_{510} - A_{750})$$

### 2.5. Transmission electron microscopy (TEM)

On the 14th day, *C. goreaui* and *D. trenchii* cells under different temperature stress were collected for transmission electron microscopy (TEM) analysis. Thirty milliliters of algal culture was centrifuged using a Sigma horizontal-rotor centrifuge at 800 ×*g* for 10 min to collect the cells. The cells were washed twice with 0.1 mol/L phosphate-buffered saline (PBS) (pH = 7.4) for 10 min each time. Then, the cells were fixed in a solution of glutaraldehyde-polyformaldehyde (2.5 %–2 %) (P1116; Beijing Solebao Technology Co., Ltd.) at room temperature in the dark for 2 h and stored at 4 °C. The fixed cells were rinsed three times with PBS for 15 min each time. Subsequently, the cells were fixed in 1 % osmium tetroxide prepared in PBS at room temperature in the dark for 2 h, followed by centrifugation and washing with PBS three times for 15 min each time. The samples were dehydrated in an ethanol gradient (30 %, 50 %, 70 %, 80 %, 95 %, and twice in 100 %, each for 20 min) and embedded in 812 embedding resin (SPI, US). The embedding blocks were sectioned using an EM UC7 ultramicrotome (Leica), stained with uranyl acetate and lead citrate, and observed and photographed using an HT7800 transmission electron microscope (Hitachi). Images were processed using ImageJ software to calculate the proportion of chloroplast area within the cells, with five cells analyzed for statistical purposes.

### 2.6. Proteomic analysis

Due to the complete bleaching of *C. goreaui* algal cells under heat stress in the later stages of the experiment, making it impossible to obtain sufficient quantity for proteomic analysis, we opted to conduct proteomic analysis on *C. goreaui* under cold stress and normal temperature, as well as on *D. trenchii* algal cells under all three cultivation conditions. Approximately 120 mL of algal culture was centrifuged at 3000 ×*g* for 5 min at 4 °C using a horizontal rotor. The pellet was washed twice with 0.1 mol/L PBS (pH = 7.4) at 4 °C for 5 min each time. After freezing in liquid nitrogen for half an hour, the samples were stored at −80 °C.

The samples were subsequently transported on dry ice to Shanghai Meiji Biomedical Technology Co., Ltd., for label-free quantitative proteomic analysis. Frozen samples were transferred into MP shaker tubes, supplemented with 1 % polyvinylpolypyrrolidone (PVPP) and an appropriate volume of BPP buffer. Samples were homogenized three times (40 s each) using a high-throughput tissue grinder. The homogenate was centrifuged at 12,000 ×*g* for 20 min at 4 °C, and the supernatant was collected. The supernatant was mixed with an equal volume of Tris-saturated phenol and vortexed at 4 °C for 10 min. After centrifugation (12,000 ×*g*, 20 min, 4 °C), the phenol phase was retained and re-extracted with an equal volume of BPP buffer. The mixture was vortexed again for 10 min and centrifuged under the same conditions. The phenol phase was then mixed with five volumes of pre-chilled ammonium acetate in methanol and incubated overnight at −20 °C to precipitate proteins. The next day, samples were centrifuged, and the supernatant was discarded. The protein pellet was washed twice with 90 % pre-chilled acetone, with centrifugation after each wash (12,000 ×*g*, 20 min, 4 °C). The final pellet was dissolved in lysis buffer (8 M urea, 1 % SDS, with protease inhibitor cocktail), sonicated on ice for 2 min, and centrifuged. The protein-containing supernatant was collected, quantified using the BCA assay, and assessed by SDS-PAGE.

After reducing, alkylating, and enzymatic digesting the protein samples, peptide desalting and quantification were performed. According to the quantification results of peptides, peptides with a concentration of 0.1 μg/μL were dissolved in mass spectrometry loading buffer (2 % acetonitrile, 0.1 % formic acid) for mass spectrometry analysis. The chromatographic separation was performed using a mobile phase system gradient composed of 2 % acetonitrile and 0.1 % formic acid (solvent A) and 80 % acetonitrile and 0.1 % formic acid (solvent B). The gradient elution of solvent B increased from 3 % at 0 min to 28 % at 45 min, then increased to 44 % at 50 min, further increased to 90 % at 55 min, and finally ended the program at 60 min, with a total chromatographic separation time of 60 min. The post-separation samples were analyzed by timsTOF Pro2 mass spectrometer (Brucker) for DDA mass spectrometry analysis. The detection mode was positive ion, with the ion source voltage set at 1.5 kV, and both MS and MS/MS were detected and analyzed using TOF. The mass spectrometry scan range was set to 100–1700 *m/z*. The data acquisition mode adopted Parallel Accumulation Serial Fragmentation (PASEF) mode.

The data analysis was performed using MaxQuant software (version 2.0.3.1). The search was based on trypsin/P digestion, with methylation of cysteine as a fixed modification, N-terminal acetylation and methionine oxidation as variable modifications, and a maximum missed cleavage value of 2. The global false discovery rate (FDR) for peptide identification was set to 0.01. The annotations of proteins from the *C. goreaui* and *D. trenchii* genome databases were used for proteomic analysis of Symbiodiniaceae. Differentially expressed proteins (DEPs) were identified based on a fold change (FC) $> 1.2$ for upregulated proteins and FC $< 0.83$ for downregulated proteins (default for label-free items). The statistical analysis of protein samples was performed using independent sample *t*-tests, with a *p* value threshold of $<0.05$ (default value for proteomics). R software was used to analyze the relationship between the differential expression of proteins and quantity and to generate PCA plots. For the proteins in the experimental samples, Blast2GO (2.5.0) software was used for Gene Ontology (GO) functional annotation, KOBAS (2.1.1) was used for Kyoto Encyclopedia of Genes and Genomes (KEGG) pathway functional annotation, hmmsca was used for Pfam functional annotation (identifying protein domains), Diamond (V0.8.3.37.99) was used for Clusters of Orthologous Groups of proteins (EggNOG) and Non-Redundant Protein Sequence Database (NR) functional annotation, and MultiLoc2 was used for Subcellular Localization (Subloc) prediction.

Enrichment analysis of the DEPs was performed for GO and KEGG pathways using Goatools for GO enrichment. Fisher's exact test was used, and the *p* values were corrected based on the Benjamini–Hochberg method. GO functions were considered significantly enriched if the corrected p value (FDR) was $<0.05$. Python-based analysis was used for KEGG pathway enrichment, with Fisher's exact test and Benjamini–Hochberg correction applied and a threshold of 0.05 for corrected p values.

### 2.7. Data statistics and analysis

The data obtained from the experiments, including the photochemical efficiency of PSII (*Fv/Fm*) and Symbiodiniaceae growth rate, were processed using Microsoft Excel. The results are presented as the mean ± standard deviation (mean ± SD). The statistical analysis was performed using SPSS 24.0 software, employing the Mann–Whitney *U* test for nonparametric analysis, with the significance level set at 0.05. Graphs were generated using Origin 2023.

## 3. Results

### 3.1. Analysis of the algal cell density and growth rate

When subjected to abnormal high-temperature stress at 34 °C, the density of the *C. goreaui* strain exhibited an overall decreasing trend, and after day 10, its value was significantly lower than the initial density ($P < 0.05$). In contrast, under normal temperature conditions (25 °C), the algal cell density increased (Supporting Information Fig. S1A). Under abnormal high-temperature stress, the density of *D. trenchii* increased, even surpassing the growth observed under normal temperature

condition (Supporting Information Fig. S1B); which also increased the growth rate analysis showed that the growth rate of *C. goreaui* decreased from 0.119 (25 °C) to −0.125 (34 °C), while that of *D. trenchii* decreased from 0.10 ± 0.01 (25 °C) to 0.066 ± 0.008 (34 °C), though the latter change was not significant ($P > 0.05$) (Fig. 1A). However, when subjected to abnormal low-temperature stress at 16 °C, the cell density of *C. goreaui* remained unchanged compared to 25 °C (Supporting Information Fig. S1A), and the growth rate was essentially 0. *D. trenchii* still exhibited slow growth, with a growth rate of 0.055 ± 0.010 (Supporting Information Fig. S1B). From the perspective of algal cell growth, *D. trenchii* was more resistant to both abnormal high- and low-temperature stress than *C. goreaui* was.

### 3.2. Analysis of the Fv/Fm value and photosynthetic pigments

Under high-temperature stress at 34 °C, the *Fv/Fm* values of *C. goreaui* gradually decreased. When the stress temperature reached 34 °C on the 4th day, the *Fv/Fm* value decreased from 0.66 ± 0.03 to 0.63 ± 0.02 and dropped to 0 on the 14th day. (Fig. 1B). However, under low-temperature stress at 16 °C, the *Fv/Fm* value of *C. goreaui* decrease during the initial 4 days of cooling from 0.61 to 0.55 but then remained mostly stable, reaching 0.54 ± 0.04 by the 14th day (Fig. 1B). Compared to *C. goreaui*, *D. trenchii* showed no significant inhibition of *Fv/Fm* under 34 °C high-temperature stress, with the value declining from 0.65 ± 0.01 to 0.58 ± 0.02 from the 1st day to the 14th day (a decrease of approximately 10 %) (Fig. 1C). However, under 16 °C low-temperature stress, the *Fv/Fm* value was significantly reduced, showing a continuous downward trend from 0.62 ± 0.01 on the 1st day to 0.32 ± 0.03 on the 14th day (a decrease of 47 %) (Fig. 1C).

When *C. goreaui* was subjected to high-temperature stress, the Chl a concentration gradually decreased, and the CAR concentration showed an overall decreasing trend. On the 14th day of 34 °C high-temperature stress, the Chl a concentration suddenly decreased by 90.22 % (Fig. 2A), while the CAR concentration decreased by only 29.56 % (0.22 ± 0.08) (Fig. 2B). However, under 16 °C low-temperature stress, the Chl a concentration exhibited an overall decreasing trend, reaching 0.42 ± 0.03 on the 14th day (a decrease of 27.16 %) (Fig. 2A). However, the CAR concentration showed an overall increasing trend, with an increase of 62.42 % (0.37 ± 0.01) on the 10th day (Fig. 2B). Compared to *C. goreaui*, *D. trenchii* showed no significant decrease in Chl a and CAR concentrations under 34 °C high-temperature stress compared to the control group; instead, both pigments showed a marked increase during the initial phase of the experiment. However, under 16 °C low-temperature stress, both Chl a and CAR concentrations gradually decreased, reaching 0.51 ± 0.05 (a decrease of 25.92 %) (Fig. 2C) and 0.42 ± 0.06 (a decrease of 6.49 %) (Fig. 2D) on the 14th day. Therefore, changes in photosynthetic pigments and *Fv/Fm* values indicate that *D. trenchii* has a tolerance to high temperature, while *C. goreaui* has a tolerance to low temperature.

### 3.3. Intracellular structure analysis of Symbiodiniaceae

The integrity of the cell structure is crucial for normal growth and reproduction. After 10 days of exposure to 34 °C high-temperature stress, *C. goreaui* exhibited morphological deformities, including shrinkage, invagination, separation of the cell wall, and disintegration of chloroplasts and chromatin, ultimately leading to cell death (Fig. 3A). However, when subjected to 16 °C low-temperature stress for 10 days, *C. goreaui* maintained an intact cell morphology, and the accumulation of lipids was observed within the cells (Fig. 3A). Due to severe cell necrosis and chloroplast disintegration caused by abnormally high temperatures, it was not possible to analyze the proportion of the chloroplast area in *C. goreaui* cells. However, under low-temperature stress conditions, the proportion of the chloroplast area in *C. goreaui* cells significantly decreased compared to that in the control group ($P < 0.05$), dropping from the normal state of 16.8 ± 3.6 % to 8.3 ± 2.0 %. In contrast to *C. goreaui*, *D. trenchii* maintained good integrity with no severe deformities after 10 days of exposure to 34 °C high-temperature stress (Fig. 3B). However, low-temperature stress resulted in cell deformities and sparse chloroplasts in *D. trenchii*. Analysis of the proportion of the chloroplast area inside the cells revealed a significant decrease under abnormal temperature stress (from 41.8 ± 2.2 % to 36.3 ± 3.0 % in the high-temperature group and from 41.8 ± 2.2 % to 30.7 ± 3.6 % in the low-temperature group). Importantly, no lipid accumulation was observed within the algal cells under these conditions (Fig. 3B). Thus, lipid accumulation inside algal cells may constitute an adaptive strategy employed by *C. goreaui* in response to abnormal low-temperature stress. At present, our results primarily reflect changes in chloroplast morphology rather than direct evidence of functional impairment. These morphological alterations may be associated with changes in photosynthetic performance.

### 3.4. Proteomic analysis

Based on the response of the two types of Symbiodiniaceae, *C. goreaui* and *D. trenchii*, to abnormal temperatures (in terms of growth rate, *Fv/Fm*, photosynthetic pigment concentration, and intracellular structural changes), it was found that the former could not maintain integrity under continuous high-temperature stress for 13 days, with severe disintegration of intracellular structures observed; in contrast, the latter exhibited greater tolerance under high-temperature stress. Additionally, after 13 days of low-temperature stress at 16 °C, both *C. goreaui* and *D. trenchii* could maintain structural integrity but showed different response patterns. Therefore, to explore the protein molecular response mechanisms of *C. goreaui* under low-temperature stress and *D. trenchii* under high/low-temperature stress, cells of *C. goreaui* subjected to low-temperature stress and normal temperature culture on the 14th day, as well as cells of *D. trenchii* subjected to high/low-temperature stress and normal temperature culture, were collected simultaneously for proteomic analysis.

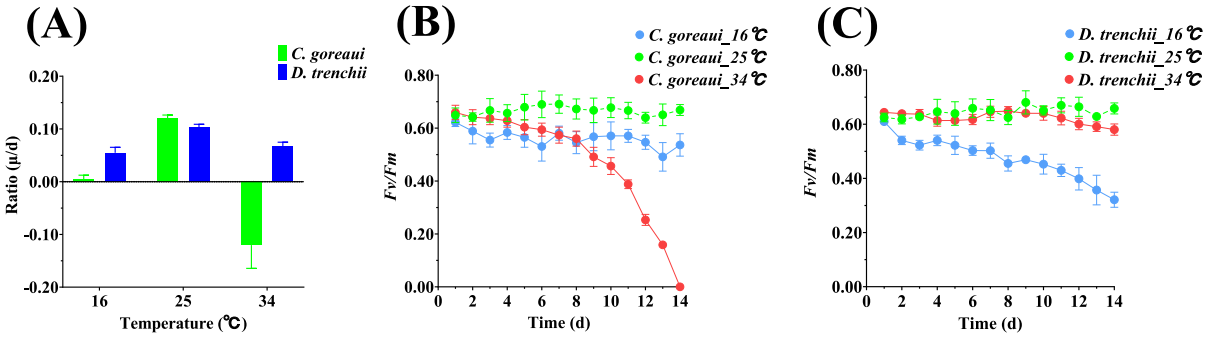


**Fig. 1.** Impact of temperature stress on the growth rate (μ) and the *Fv/Fm* value of Symbiodiniaceae. (A) Impact of temperature stress on the growth rate (μ) of *C. goreaui* and *D. trenchii*. (B) Influence of temperature stress on the *Fv/Fm* value of *C. goreaui*. (C) Influence of temperature stress on the *Fv/Fm* value of *D. trenchii*.

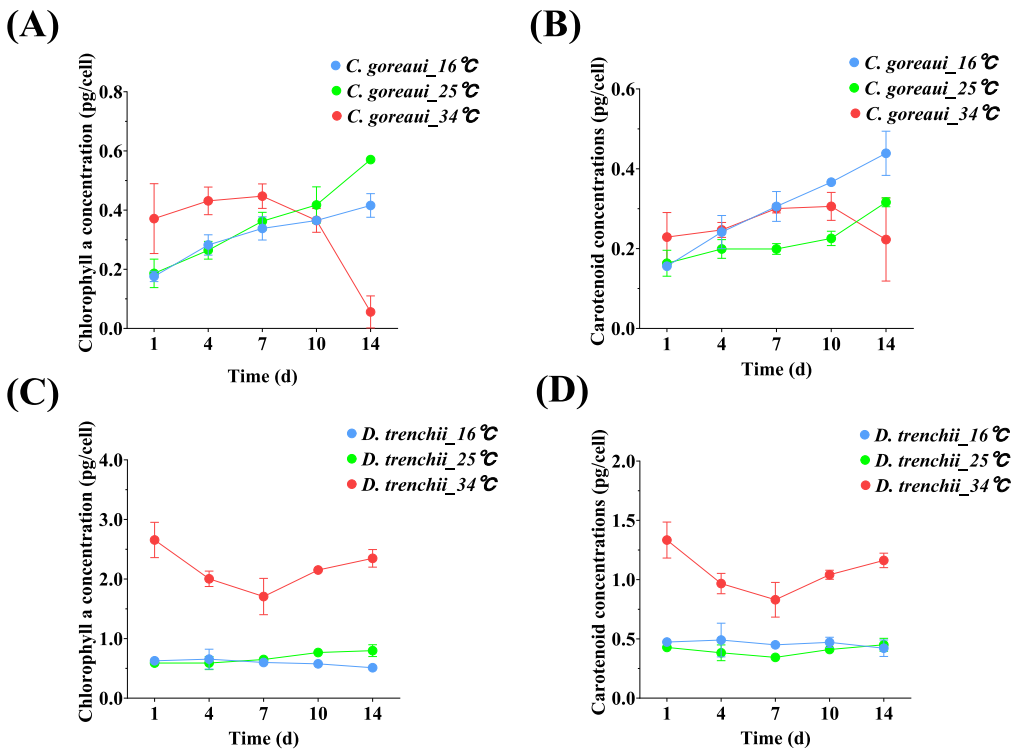


**Fig. 2.** Changes in the photosynthetic pigments of Symbiodiniaceae under high/low-temperature stress. (A) Changes in the Chl a Concentration of *C. goreaui* under High- and Low-Temperature Stress. (B) Changes in the CAR Concentration of *C. goreaui* under High- and Low-Temperature Stress. (C) Changes in the Chl a Concentration of *D. trenchii* under High- and Low-Temperature Stress. (D) Changes in the CAR Concentration of *D. trenchii* under High and Low-Temperature Stress.

With MaxQuant software used for database search analysis, a total of 15 samples yielded 32,461 spectra, with 31,339 unique spectra matching 4782 peptides and 1336 proteins. The number of proteins assembled into different protein groups in all the samples was 1030 (Supporting Information Fig. S2A). Among all the detected proteins, 893 were annotated by EggNOG, 856 by GO, 746 by KEGG, 883 by Pfam, and 1030 by subcellular localization (Subloc) (Supporting Information Fig. S2B). Specific functional annotations of all proteins are provided in Supporting Information Figs. S3-S7. Among the detected proteins, significant DEPs were recovered under low-temperature stress in *C. goreaui* compared to the control group, low-temperature stress in *D. trenchii* compared to the control group, and high-temperature stress in *D. trenchii* compared to the control group; the numbers of uniquely expressed proteins were 95, 183, and 179, and the total numbers of significant DEPs were 237, 267, and 268, respectively (Fig. 4A, B, C). The results for the upregulated and downregulated proteins are shown in Fig. 4D. PCA indicated that the effect of species identity (PC1 45.5 %) was greater than the effect of abnormal temperature (PC2 14.5 %) on these species (Fig. 4E). Similarly, within the same species, high/low-temperature stresses did not affect them to the same extent (Supporting Information Fig. S8).

### 3.4.1. GO enrichment analysis

We conducted enrichment analysis of DEPs in three major GO categories: Biological Processes (BP), Cellular Components (CC), and Molecular Functions (MF). The results revealed that under low-temperature stress, the top 10 significantly enriched GO terms for DEPs in *C. goreaui* were (Fig. 5): purine-containing compound biosynthetic process; phosphoric ester hydrolase activity; IMP metabolic process; 4 iron, 4 sulfur cluster binding; cellular metabolic compound salvage; metal ion binding; metal cluster binding; iron–sulfur cluster binding; ribonucleotide biosynthetic process; ribose phosphate biosynthetic process.

Under low-temperature stress, the top 10 significantly enriched GO terms for DEPs in *D. trenchii* were (Fig. 5): nuclear protein-containing complex; spliceosomal snRNP complex; small nuclear ribonucleoprotein complex; Sm-like protein family complex; U2 snRNP; ribonucleoprotein complex subunit organization; ribonucleoprotein complex assembly; RNA binding; spliceosomal complex assembly; protein–containing complex assembly.

Under high-temperature stress, the top 10 significantly enriched GO terms for DEPs in *D. trenchii* were (Fig. 5): ubiquitin-like protein transferase activity; response to inorganic substance; sulfur compound metabolic process; thioester biosynthetic process; purine nucleoside bisphosphate biosynthetic process; nucleoside bisphosphate biosynthetic process; acyl–CoA biosynthetic process; ribonucleoside bisphosphate biosynthetic process; organic hydroxy compound biosynthetic process; response to metal ion.

### 3.4.2. KEGG enrichment analysis

Likewise, to further understand the impact of abnormal temperature stress on Symbiodiniaceae cells and their related pathways, pathway enrichment analysis was conducted for the top 10 most significantly enriched KEGG pathways. An adjusted *P* value (*P*adjust) $<0.05$ was considered to indicate a significantly enriched KEGG pathway function. The results indicated that under abnormal low-temperature stress, the DEPs were significantly enriched in *C. goreaui* were (Fig. 6): Citrate cycle (TCA cycle); ribosome; inositol phosphate metabolism; oxidative phosphorylation; spliceosome; purine metabolism; butanoate metabolism; nitrogen metabolism; valine, leucine and isoleucine degradation; glutathione metabolism.

When subjected to abnormal low-temperature stress, *D. trenchii* exhibited significant enrichment of DEPs in pathways such as Spliceosome; ribosome biogenesis in eukaryotes; peroxisome; proteasome; plant–pathogen interaction; nicotinate and nicotinamide metabolism; glycerophospholipid metabolism; biosynthesis of cofactors; arginine biosynthesis; propanoate metabolism (Fig. 6).

For *D. trenchii* under abnormally high-temperature stress, the DEPs were significantly enriched in RNA degradation; pantothenate and CoA

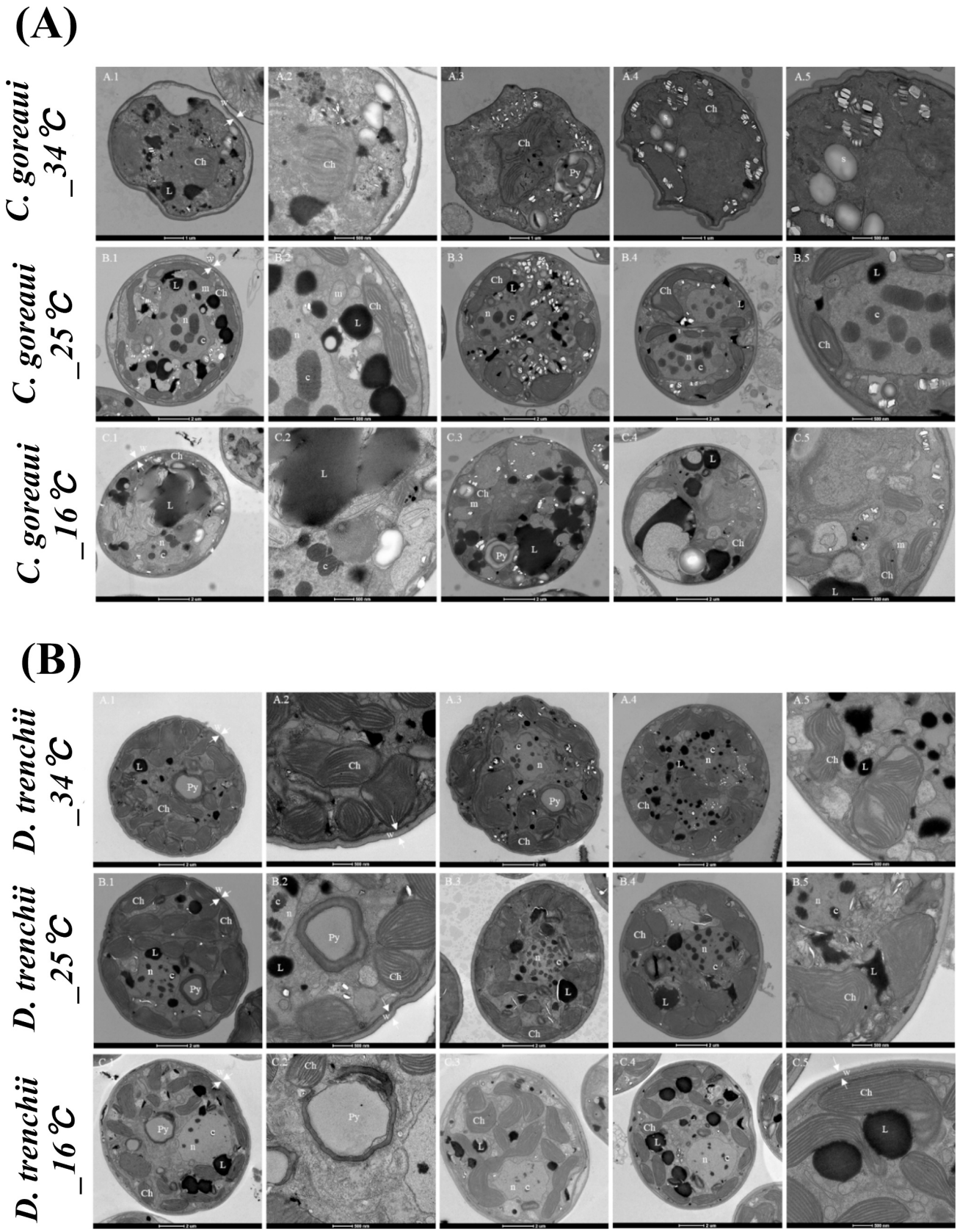


**Fig. 3.** (A). Ultrastructure of *C. goreaui*; (B). Ultrastructure of *D. trenchii* n: nucleus; c: chromosome; Ch: chloroplast; Py: pyrenoid; m: mitochondrion; s: starch; a: accumulation body; w: cell wall (paired arrows indicate cell wall thickness); v: vacuole.

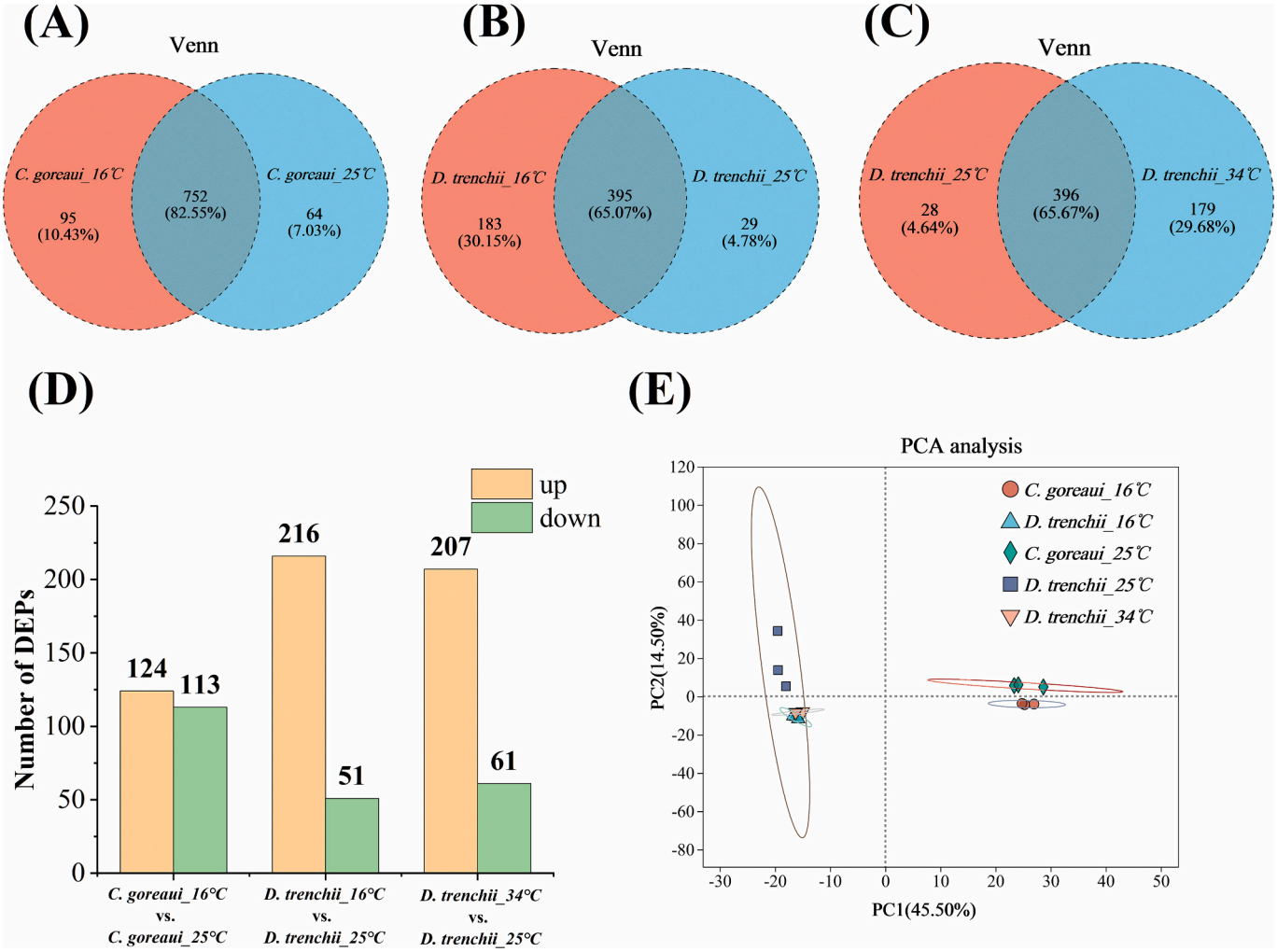


**Fig. 4.** (A) Specific protein expression in *C. goreaui* induced by abnormal low-temperature stress. (B) Specific protein expression in *D. trenchii* induced by abnormal low-temperature stress (C) Specific protein expression in *D. trenchii* induced by abnormal high-temperature stress. (D) Differential protein expression under different conditions. (E) PCA.

biosynthesis; thiamine metabolism; fatty acid biosynthesis; fatty acid degradation; alanine, aspartate and glutamate metabolism; fructose and mannose metabolism; nucleotide metabolism; porphyrin metabolism; glycerophospholipid metabolism (Fig. 6).

## 4. Discussion

The molecular basis of the physiological response of coral-Symbiodiniaceae symbiosis to environmental stress has been investigated mainly through transcriptomics and metabolomics. Various gene expression methods have been utilized to assess the genetic responses of corals to stress. Although these studies have made significant progress in enhancing our understanding of the molecular responses of coral hosts, symbiotic microorganisms, and the entire system under environmental stress, they do not necessarily represent the true phenotypes at the protein level in these cells. The proteome provides a more accurate reflection of biological functions since proteins typically have higher abundances than transcripts and have longer half-lives inside cells [32]. The presence of Symbiodiniaceae plays a crucial role in the survival of coral hosts, and temperature fluctuations can lead to changes in algal density, photosynthetic pigment concentration, photochemical efficiency of PSII, photosynthetic capacity, and the xanthophyll cycle [33]. It is well established that both thermal and cold anomalies can drive coral bleaching (i.e., loss of symbionts) and increase mortality rates [34–36]. Heat stress and cold stress primarily exert adverse effects on photosynthesis but can induce enhanced photoprotective mechanisms, thereby mitigating the impact of transient exposure on photosynthetic processes [33]. However, these temperature extremes affect distinct physiological processes and may involve trade-offs in stress tolerance [37]. In this study, the physiological characteristics and molecular stress response mechanisms of *C. goreaui* and *D. trenchii* were investigated under abnormally high/low temperatures during the same period. Both cold and heat stress had negative effects on Symbiodiniaceae, this research contributes to elucidating the adaptive strategies of different species of Symbiodiniaceae to different temperatures: for *C. goreaui*, high-temperature stress had a greater impact than low-temperature stress, while the opposite was observed for *D. trenchii* under stress.

### *4.1. Physiological and proteomic responses of two Symbiodiniaceae species to high temperature stress*

Elevated temperatures are known to cause PSII photoinhibition and impair photodamage repair mechanisms in Symbiodiniaceae [38]. These impairments suppress metabolic performance and represent a primary driver of thermal bleaching in corals [38–41]. Previous studies have reported damage to coral hosts under prolonged exposure to 34 °C (12h) or extended periods of extreme temperature stress at 36 °C, leading to apoptosis or necrosis in Symbiodiniaceae cells, which are

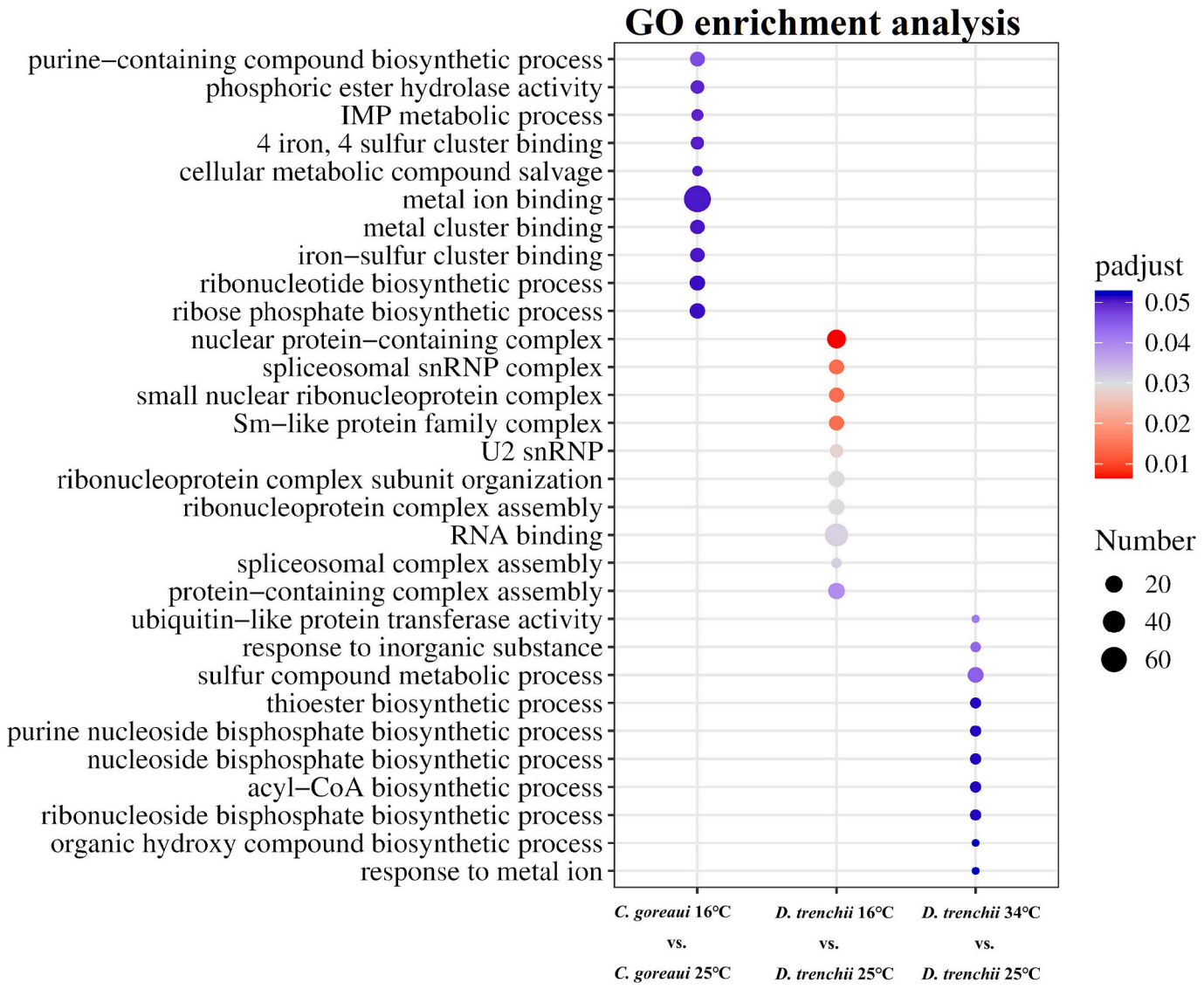


**Fig. 5.** GO enrichment analysis of DEPs in Symbiodiniaceae under abnormal temperature stress. (The x-axis represents different groups, the y-axis represents the GO term, and the size of the bubbles is proportional to the number of proteins enriched in this GO term.)

subsequently expelled [42,43].

Under high-temperature stress (34 °C), *Cladocopium goreaui* exhibited typical thermosensitive characteristics [9], including a significant decline in cell density (Supporting Information S1A), negative growth rate ($\mu < 0$) (Fig. 1A), a sharp reduction in the *Fv/Fm* value (Fig. 1B), and fluctuating levels of Chl a and CARs (initial increase followed by decrease; Fig. 2A, B). Moreover, its cellular structure was severely damaged, with disintegration of chloroplast morphology (Fig. 3A), indicating a pronounced impairment of photosynthesis [44]. These physiological deteriorations are consistent with previously described heat-induced photosynthetic inhibition and oxidative stress damage [45–48]. Heat stress suppresses D1 protein repair and destabilizes PSII reaction centers, contributing to the observed *Fv/Fm* decline [49,50]. Additionally, pigment degradation is a known photoprotective strategy that limits Reactive oxygen species (ROS) accumulation [51,52]. Chloroplast structures are disrupted prior to widespread oxidative damage under thermal stress, and diminished photosynthesis forces Symbiodiniaceae chloroplasts to reroute electrons via the Mehler reaction [53].

In contrast, *Durusdinium trenchii* demonstrated higher thermal tolerance under the same stress conditions [54,55]. Although its growth rate was reduced compared to the control (Fig. 1A), cell density increased (Supporting Information S1B), *Fv/Fm* showed only a modest decline (Fig. 1B), pigment concentrations remained relatively high (Fig. 2C, D), and cell structures, including chloroplasts, remained intact (Fig. 3B), indicating a more stable photosynthetic and metabolic function under heat stress. Proteomic analysis supported these findings. GO enrichment revealed significant upregulation of ATP-dependent protein-folding chaperones such as *HSP70* (Fig. 5), suggesting enhanced proteostasis mechanisms to counteract heat-induced protein denaturation [56–58]. KEGG pathway analysis also showed strong activation of endocytosis and ubiquitin-mediated proteolysis pathways (Fig. 6), indicating an enhanced cellular response to misfolded proteins [48,59,60]. Meanwhile, protein expression associated with photosystem I (PSI), the Calvin cycle, and pigment biosynthesis was downregulated (Figs. 5, 6), implying reduced light absorption and electron transport, which may lower the synthesis of photosynthetic products [61]. Proteins involved in chloroplast lipid biosynthesis, such as acetyl-CoA carboxylase (ACC) and ω-6 fatty acid desaturase (FAD6), were upregulated (Fig. 5). ACC catalyzes the carboxylation of acetyl-CoA in the rate-limiting step of fatty acid biosynthesis, potentially increasing unsaturated fatty acid content to enhance membrane fluidity and chloroplast stability [62]. High expression of proteins such as 4-hydroxyphenylpyruvate dioxygenase (HPPD) and 2-methyl-6-phytyl-1,4-hydroquinone methyltransferase (MPBQ-MT) was observed in the biosynthesis of

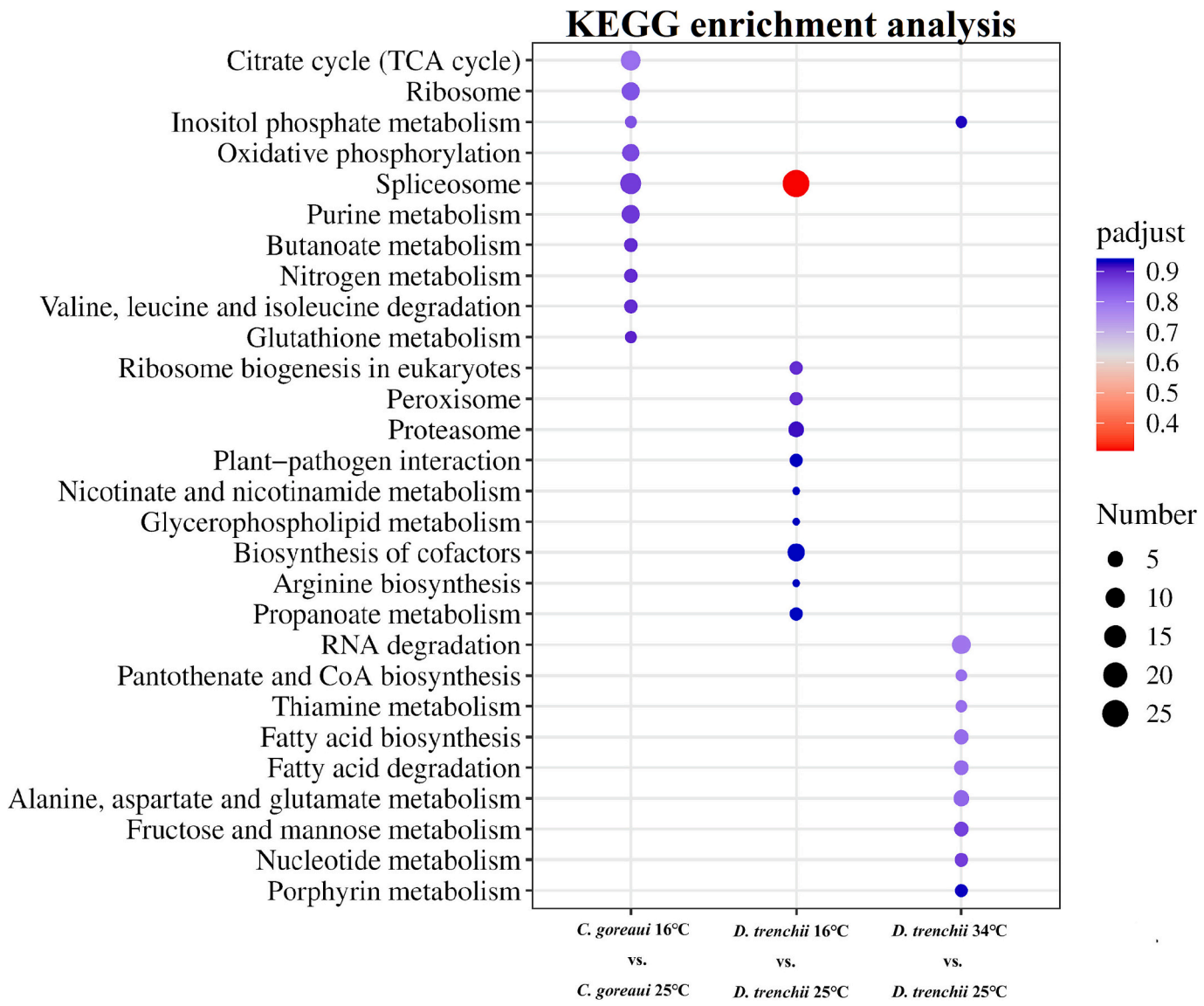


**Fig. 6.** KEGG pathway analysis of DEPs in Symbiodiniaceae under abnormal temperature stress. (The x-axis represents different groups, the y-axis represents the KEGG pathway, and the size of the bubbles indicates the number of proteins enriched in the KEGG pathway.)

plastoquinones and other terpenoid quinones under heat stress (Figs. 5, 6). These pathways are critical for α-tocopherol (vitamin E) synthesis, a lipid-soluble antioxidant that scavenges singlet oxygen within chloroplasts, protects membrane lipids from peroxidation, and stabilizes photosynthetic complexes. The quinone form of α-tocopherol also integrates into the thylakoid electron transport chain, providing additional photoprotection [63]. In addition, biosynthetic pathways for macromolecules and organic compounds were downregulated, possibly reflecting a strategic reallocation of resources toward stress response mechanisms [64].

In summary, *C. goreaui* exhibited extreme sensitivity to heat stress, displaying a characteristic "photoinhibition–cell collapse" pattern, while *D. trenchii* showed strong thermal adaptation through enhanced chaperone activity, protein degradation systems, and pigment stability. These differential responses are consistent with previous studies on the evolutionary thermal tolerance and species-specific adaptation of Symbiodiniaceae [10,65–69].

### 4.2. Physiological and proteomic responses of two Symbiodiniaceae species to low temperature stress

Both high and low temperatures have been shown to accelerate photoinhibition (fixing $CO_2$ by severely limiting photosynthesis) [70–72]. The structural integrity of symbiont chloroplasts is essential for maintaining photosynthetic capacity under thermal stress. Similarly, exposure to cold stress also reduces the *Fv/Fm* in Symbiodiniaceae, potentially leading to photoinhibition and photodamage [36,61]. It negatively affects photosynthesis by reducing chlorophyll fluorescence quantum yield, weakening the activity of carbon fixation enzymes [33,36,61,73], and lowering membrane fluidity [61].

Under low temperature stress (16 °C), neither species exhibited severe physiological damage. Although cell density growth slowed during the later stages of the experiment, the overall μ values remained positive (Fig. 1A). Cellular structures remained intact (Fig. 3), and concentrations of Chl a and CARs showed no significant differences from the control group ($P > 0.05$; Fig. 2), suggesting a degree of cold tolerance in both species. However, both experienced declines in the *Fv/Fm* value, with a more pronounced decrease in *D. trenchii* than in *C. goreaui* (Fig. 1B), indicating that despite stable pigment content, PSII function

was impaired in both, and *C. goreaui* may be better adapted to cold stress [9]. Proteomic analysis further revealed the molecular basis of this adaptation. In *C. goreaui*, GO-enriched pathways upregulated under cold stress included metal ion transport, glutathione biosynthesis, and α-ketoglutarate dehydrogenase activity, indicating the activation of redox homeostasis and mitochondrial TCA cycle pathways [74,75]. Glutathione synthesis can help scavenge cold-induced ROS and maintain intracellular redox balance [76]. KEGG analysis also showed significant downregulation of fatty acid, pyruvate, and nicotinamide metabolism, supporting a strategy of metabolic suppression [77].

In *D. trenchii*, cold stress predominantly triggered extensive upregulation of RNA splicing-related pathways, including the spliceosome, snRNP complexes, and mRNA splicing (significant in both GO and KEGG enrichment), suggesting active post-transcriptional regulation and rapid adjustment to temperature changes via splicing machinery [78–80]. Concurrently, pathways related to carbohydrate biosynthesis and the electron transport chain were downregulated, indicating reduced energy metabolism under cold conditions [81]. $NAD^+$-dependent GPD1 was upregulated in *C. goreaui*, and FAD-dependent GPD2 was upregulated in *D. trenchii*. Both enzymes catalyze the conversion of dihydroxyacetone phosphate (DHAP) to glycerol-3-phosphate (G3P), providing the glycerol backbone for triacylglycerol (TAG) synthesis [82]. The fatty acid β-oxidation enzyme ACAA1 was also upregulated in *D. trenchii*, which is associated with reduced lipid synthesis and decreased TAG accumulation, indicating a metabolic shift from lipid storage to utilization [83].

In conclusion, *C. goreaui* demonstrated a degree of cold tolerance by activating antioxidant and metabolic homeostasis mechanisms, while *D. trenchii*, despite being more photosynthetically sensitive, showed active post-transcriptional regulation through enhanced spliceosome-related protein expression. These strategic differences reflect distinct priorities in resource allocation and regulatory focus in response to cold stress.

## 5. Conclusion

Many ecological studies on coral reefs have shown that the density of Symbiodiniaceae *in hospite* is lower in warmer summers and higher in winters [84]. This patterns may be explained by the impact of low temperatures on Symbiodiniaceae, with the weaken photosynthesis and decrease nutrient supply to corals [36,61,85]. However, the relationship between the density of Symbiodiniaceae and metabolism are nuanced [86]. For instance, an increase in nutrients within a certain range may lead to an increase in the density of Symbiodiniaceae [87]. But, when the nutrient level exceeds a certain threshold, the density of Symbiodiniaceae may actually decrease [87]. Recent transcriptomics and metabolomics studies demonstrate the importance of nutrients in host-symbiont interactions [58,88–91], they can provide insights into the molecular mechanisms underlying the changes in Symbiodiniaceae density and metabolism.

This study elucidates the distinct stress-response strategies of two Symbiodiniaceae species, *Cladocopium goreaui* and *Durusdinium trenchii*, under extreme temperature conditions. At elevated temperatures (34 °C), *C. goreaui* exhibited marked reductions in growth, photosynthetic efficiency, and cellular integrity, indicating pronounced thermal sensitivity. In contrast, *D. trenchii* maintained relatively stable physiological functions while activating multiple protective mechanisms, including chaperone-mediated protein folding and antioxidant biosynthesis. Under cold stress (16 °C), both species displayed minimal physiological impairment; however, *C. goreaui* appeared more cold-tolerant through modulation of redox homeostasis and TCA cycle activity, whereas *D. trenchii* responded via enhanced post-transcriptional regulation involving spliceosome-related pathways. These results highlight species-specific thermal adaptation mechanisms and provide new insights into the resilience of coral-algal symbioses in the context of climate change.

## CRediT authorship contribution statement

**Jiayuan Liang:** Writing – review & editing, Writing – original draft. **Liangyun Qin:** Writing – review & editing, Writing – original draft, Methodology, Investigation, Formal analysis, Data curation. **Li Zhang:** Writing – review & editing, Writing – original draft, Investigation, Data curation. **Yongqian Xu:** Methodology, Investigation. **Tianyi Niu:** Methodology, Investigation. **Zhicong Li:** Methodology, Investigation. **Yating Yang:** Methodology, Investigation. **Zhuqing Liang:** Methodology, Investigation. **Kefu Yu:** Funding acquisition. **Sanqiang Gong:** Data curation.

## Declaration of competing interest

All authors declare no conflict of interest.

## Acknowledgements

This work was supported by the National Natural Science Foundation of China (42030502 and 42090041), and the Self-Topic Project of Guangxi Laboratory on the Study of Coral Reefs in the South China Sea (GXLSCRSCS2023101).

## Appendix A. Supplementary data

Supplementary data to this article can be found online at https://doi.org/10.1016/j.algal.2025.104187.

## Data availability

Data will be made available on request.

## References

[1] L. Muscatine, L.R. McCloskey, R.E. Marian, Estimating the daily contribution of carbon from zooxanthellae to coral animal respiration, Limnol. Oceanogr. 26 (1981) 601–611.
[2] P.G. Falkowski, Z. Dubinsky, L. Muscatine, J.W. Porter, Light and the bioenergetics of a symbiotic coral, BioScience 34 (1984) 705–709.
[3] M.S. Roth, The engine of the reef: photobiology of the coral-algal symbiosis, Front. Microbiol. 5 (2014).
[4] D.G. Bourne, K.M. Morrow, N.S. Webster, Insights into the coral microbiome: underpinning the health and resilience of reef ecosystems, in: S. Gottesman (Ed.), Annual Review of Microbiology Vol 70, 2016, pp. 317-+.
[5] S.L. Coles, Reef corals occurring in a highly fluctuating temperature environment at Fahal Island, Gulf of Oman (Indian Ocean), Coral Reefs 16 (1997) 269–272.
[6] P. Craig, C. Birkeland, S. Belliveau, High temperatures tolerated by a diverse assemblage of shallow-water corals in American Samoa, Coral Reefs 20 (2001) 185–189.
[7] N.M. Boulotte, S.J. Dalton, A.G. Carroll, P.L. Harrison, H.M. Putnam, L.M. Peplow, M.J.H. van Oppen, Exploring the *Symbiodinium* rare biosphere provides evidence for symbiont switching in reef-building corals, ISME J. 10 (2016) 2693–2701.
[8] T.A. Oliver, S.R. Palumbi, Many corals host thermally resistant symbionts in high-temperature habitat, Coral Reefs 30 (2011) 241–250.
[9] R. Rowan, Coral bleaching: thermal adaptation in reef coral symbionts, Nature 430 (2004) 742.
[10] R. Berkelmans, M.J.H. van Oppen, The role of zooxanthellae in the thermal tolerance of corals: a 'nugget of hope' for coral reefs in an era of climate change, Proc. R. Soc. B Biol. Sci. 273 (2006) 2305–2312.
[11] D. Abrego, K.E. Ulstrup, B.L. Willis, M.J.H. van Oppen, Species–specific interactions between algal endosymbionts and coral hosts define their bleaching response to heat and light stress, Proc. R. Soc. B Biol. Sci. 275 (2008) 2273–2282.
[12] T.C. LaJeunesse, J.E. Parkinson, P.W. Gabrielson, H.J. Jeong, J.D. Reimer, C. R. Voolstra, S.R. Santos, Systematic revision of Symbiodiniaceae highlights the antiquity and diversity of coral endosymbionts, Curr. Biol. 28 (2018) 2570.
[13] T.C. LaJeunesse, D.T. Pettay, E.M. Sampayo, N. Phongsuwan, B. Brown, D. O. Obura, O. Hoegh-Guldberg, W.K. Fitt, Long-standing environmental conditions, geographic isolation and host–symbiont specificity influence the relative ecological dominance and genetic diversification of coral endosymbionts in the genus *Symbiodinium*, J. Biogeogr. 37 (2010) 785–800.
[14] T.C. LaJeunesse, R. Smith, M. Walther, J. Pinzon, D.T. Pettay, M. McGinley, M. Aschaffenburg, P. Medina-Rosas, A.L. Cupul-Magana, A. Lopez Perez, H. Reyes-Bonilla, M.E. Warner, Host-symbiont recombination versus natural selection in the response of coral-dinoflagellate symbioses to environmental disturbance, Proc. R. Soc. B Biol. Sci. 277 (2010) 2925–2934.

[15] D.P. Manzello, M.V. Matz, I.C. Enochs, L. Valentino, R.D. Carlton, G. Kolodziej, X. Serrano, E.K. Towle, M. Jankulak, Role of host genetics and heat-tolerant algal symbionts in sustaining populations of the endangered coral *Orbicella faveolata* in the Florida keys with ocean warming, Glob. Chang. Biol. 25 (2019) 1016–1031.
[16] B. Chen, Spatial Changes of Coral Miceobiome and Environmental Adaption Mechanism in the South Chine Sea, Guangxi University, 2021.
[17] D.M. Baker, J.P. Andras, A.G. Jordán-Garza, M.L. Fogel, Nitrate competition in a coral symbiosis varies with temperature among *Symbiodinium* clades, ISME J. 7 (2013) 1248–1251.
[18] K.D. Hoadley, D.T. Pettay, A. Lewis, D. Wham, C. Grasso, R. Smith, D.W. Kemp, T. LaJeunesse, M.E. Warner, Different functional traits among closely related algal symbionts dictate stress endurance for vital Indo-Pacific reef-building corals, Glob. Chang. Biol. 27 (2021) 5295–5309.
[19] B. Chen, K. Yu, J. Liang, W. Huang, G. Wang, H. Su, Z. Qin, X. Huang, Z. Pan, W. Luo, Y. Luo, Y. Wang, Latitudinal variation in the molecular diversity and community composition of Symbiodiniaceae in coral from the South China Sea, Front. Microbiol. 10 (2019).
[20] S. Keshavmurthy, K.-H. Tang, C.-M. Hsu, C.-H. Gan, C.-Y. Kuo, K. Soong, H.-N. Chou, C.A. Chen, *Symbiodinium* spp. associated with scleractinian corals from Dongsha Atoll (Pratas), Taiwan, in the South China Sea, PeerJ 5 (2017) e2871.
[21] B. Chen, K. Yu, J. Liang, W. Huang, G. Wang, H. Su, Z. Qin, X. Huang, Z. Pan, W. Luo, Y. Luo, Y. Wang, Latitudinal variation in the molecular diversity and community composition of Symbiodiniaceae in coral from the South China Sea, Front. Microbiol. 10 (2019) 1278.
[22] E.M. Sampayo, T. Ridgway, P. Bongaerts, O. Hoegh-Guldberg, Bleaching susceptibility and mortality of corals are determined by fine-scale differences in symbiont type, Proc. Natl. Acad. Sci. USA 105 (2008) 10444–10449.
[23] M.D. Ahles, Some Aspects of the Morphology and Physiology of *Symbiodinium microadriaticum*, Fordham University, 1967.
[24] R.A. Kinzie, P.L. Jokiel, R. York, Effects of light of altered spectral composition on coral zooxanthellae associations and on zooxanthellae *in vitro*, Mar. Biol. 78 (1984) 239–248.
[25] J.J. Lee, M.E. McEnery, J.R. Garrison, Experimental studies of larger foraminifera and their symbionts from the Gulf of Elat on the Red Sea, J. Foraminifer. Res. 10 (1980) 31–47.
[26] L. Qin, Y. Xu, J. Chen, T. Niu, K. Yu, J. Liang, Optimization of in vitro culture method for zooxanthellae associated with reef-building corals, Acta Microbiol Sin. 63 (2023) 1658–1671.
[27] Y.U. Kefu, J. Mingxing, C. Zhiqiang, C. Tegu, Latest forty two years' sea surface temperature change of Weizhou Island and its influence on coral reef ecosystem, Chin. J. Appl. Ecol. (2004) 506–510.
[28] J.E.N. Veron, P.R. Minchin, Correlations between sea surface temperature, circulation patterns and the distribution of hermatypic corals of Japan, Cont. Shelf Res. 12 (1992) 835–857.
[29] W. Huang, L. Meng, Z. Xiao, R. Tan, E. Yang, Y. Wang, X. Huang, K. Yu, Heat-tolerant intertidal rock pool coral *Porites lutea* can potentially adapt to future warming, Mol. Ecol. 33 (2024) e17273.
[30] Y.P. Guo, D.P. Guo, H.F. Zhou, M.J. Hu, Y.G. Shen, Photoinhibition and xanthophyll cycle activity in bayberry (*Myrica rubra*) leaves induced by high irradiance, Photosynthetica 44 (2006) 439–446.
[31] R.J. Ritchie, Consistent sets of spectrophotometric chlorophyll equations for acetone, methanol and ethanol solvents, Photosynth. Res. 89 (2006) 27–41.
[32] A.J. Weston, W.C. Dunlap, J.M. Shick, A. Klueter, K. Iglic, A. Vukelic, A. Starcevic, M. Ward, M.L. Wells, C.G. Trick, P.F. Long, A profile of an endosymbiont-enriched fraction of the coral *Stylophora pistillata* reveals proteins relevant to microbial-host interactions, Mol. Cell. Proteomics 11 (2012).
[33] M.S. Roth, R. Goericke, D.D. Deheyn, Cold induces acute stress but heat is ultimately more deleterious for the reef-building coral *Acropora yongei*, Sci. Rep. 2 (2012).
[34] P.L. Jokiel, S.L. Coles, Response of Hawaiian and other Indo-Pacific reef corals to elevated temperature, Coral Reefs 8 (1990) 155–162.
[35] T.C. LaJeunesse, H. Reyes-Bonilla, M.E. Warner, Spring "bleaching" among *Pocillopora* in the Sea of Cortez, Eastern Pacific, Coral Reefs 26 (2007) 265–270.
[36] T. Saxby, W.C. Dennison, O. Hoegh-Guldberg, Photosynthetic responses of the coral *Montipora digitata* to cold temperature stress, Mar. Ecol. Prog. Ser. 248 (2003) 85–97.
[37] M.S. Roth, D.D. Deheyn, Effects of cold stress and heat stress on coral fluorescence in reef-building corals, Sci. Rep. 3 (2013) 1421.
[38] M.E. Warner, W.K. Fitt, G.W. Schmidt, Damage to photosystem II in symbiotic dinoflagellates: a determinant of coral bleaching, Proc. Natl. Acad. Sci. 96 (1999) 8007–8012.
[39] S. Takahashi, T. Nakamura, M. Sakamizu, R.v. Woesik, H. Yamasaki, Repair machinery of symbiotic photosynthesis as the primary target of heat stress for reef-building corals, Plant Cell Physiol. 45 (2004) 251–255.
[40] S. Takahashi, S. Whitney, S. Itoh, T. Maruyama, M. Badger, Heat stress causes inhibition of the *de novo* synthesis of antenna proteins and photobleaching in cultured *Symbiodinium*, Proc. Natl. Acad. Sci. USA 105 (2008) 4203–4208.
[41] D.J. Smith, D.J. Suggett, N.R. Baker, Is photoinhibition of zooxanthellae photosynthesis the primary cause of thermal bleaching in corals? Glob. Chang. Biol. 11 (2004) 1–11.
[42] P.W. Sammarco, K.B. Strychar, Responses to high seawater temperatures in zooxanthellate octocorals, PLoS One 8 (2013).
[43] K.B. Strychar, P.W. Sammarco, Exaptation in corals to high seawater temperatures: low concentrations of apoptotic and necrotic cells in host coral tissue under bleaching conditions, J. Exp. Mar. Biol. Ecol. 369 (2009) 31–42.
[44] C. Ferrier-Pagès, C. Rottier, E. Beraud, O. Levy, Experimental assessment of the feeding effort of three scleractinian coral species during a thermal stress: effect on the rates of photosynthesis, J. Exp. Mar. Biol. Ecol. 390 (2010) 118–124.
[45] M.P. Lesser, Experimental biology of coral reef ecosystems, J. Exp. Mar. Biol. Ecol. 300 (2004) 217–252.
[46] D. Tchernov, M.Y. Gorbunov, C. de Vargas, S. Narayan Yadav, A.J. Milligan, M. Häggblom, P.G. Falkowski, Membrane lipids of symbiotic algae are diagnostic of sensitivity to thermal bleaching in corals, Proc. Natl. Acad. Sci. 101 (2004) 13531–13535.
[47] T. Krueger, T.D. Hawkins, S. Becker, S. Pontasch, S. Dove, O. Hoegh-Guldberg, W. Leggat, P.L. Fisher, S.K. Davy, Differential coral bleaching-contrasting the activity and response of enzymatic antioxidants in symbiotic partners under thermal stress, Comp. Biochem. Physiol. A Mol. Integr. Physiol. 190 (2015) 15–25.
[48] C.A. Oakley, M.F. Ameismeier, L. Peng, V.M. Weis, A.R. Grossman, S.K. Davy, Symbiosis induces widespread changes in the proteome of the model cnidarian *Aiptasia*, Cell. Microbiol. 18 (2016) 1009–1023.
[49] S. Takahashi, N. Murata, How do environmental stresses accelerate photoinhibition? Trends Plant Sci. 13 (2008) 178–182.
[50] R.J. Jones, O. Hoegh-Guldberg, A.W.D. Larkum, U. Schreiber, Temperature-induced bleaching of corals begins with impairment of the $CO_2$ fixation mechanism in zooxanthellae, Plant Cell Environ. 21 (1998) 1219–1230.
[51] E.S. McGinty, J. Pieczonka, L.D. Mydlarz, Variations in reactive oxygen release and antioxidant activity in multiple *Symbiodinium* types in response to elevated temperature, Microb. Ecol. 64 (2012) 1000–1007.
[52] O. Ladrière, P. Compère, D. Nicole, P. Vandewalle, M. Poulicek, Morphological alterations of zooxanthellae in bleached cnidarian hosts, Cah. Biol. Mar. 49 (2008) 215–227.
[53] C.A. Downs, K.E. McDougall, C.M. Woodley, J.E. Fauth, R.H. Richmond, A. Kushmaro, S.W. Gibb, Y. Loya, G.K. Ostrander, E. Kramarsky-Winter, Heat-stress and light-stress induce different cellular pathologies in the symbiotic dinoflagellate during coral bleaching, PLoS One 8 (2013).
[54] R.N. Silverstein, R. Cunning, A.C. Baker, Tenacious D: *Symbiodinium* in clade D remain in reef corals at both high and low temperature extremes despite impairment, J. Exp. Biol. 220 (2017) 1192–1196.
[55] A.C. Baker, C.J. Starger, T.R. McClanahan, P.W. Glynn, Corals' adaptive response to climate change, Nature 430 (2004), 741-741.
[56] M.E. Feder, G.E. Hofmann, Heat-shock proteins, molecular chaperones, and the stress response: evolutionary and ecological physiology, Annu. Rev. Physiol. 61 (1999) 243–282.
[57] R. Rosenzweig, N.B. Nillegoda, M.P. Mayer, B. Bukau, The Hsp70 chaperone network, Nat. Rev. Mol. Cell Biol. 20 (2019) 665–680.
[58] T. Li, X. Lin, L. Yu, S. Lin, I.B. Rodriguez, T.-Y. Ho, RNA-seq profiling of *Fugacium kawagutii* reveals strong responses in metabolic processes and symbiosis potential to deficiencies of iron and other trace metals, Sci. Total Environ. 705 (2020) 135767.
[59] M.H. Glickman, A. Ciechanover, The ubiquitin-proteasome proteolytic pathway: destruction for the sake of construction, Physiol. Rev. 82 (2002) 373–428.
[60] L. Zhang, J. Xing, J. Lin, At the intersection of exocytosis and endocytosis in plants, New Phytol. 224 (2019) 1479–1489.
[61] D.J. Thornhill, D.W. Kemp, B.U. Bruns, W.K. Fitt, G.W. Schmidt, Correspondence between cold tolerance and temperate biogeography in a Western Atlantic *Symbiodinium* (Dinophyta) lineage[1], J. Phycol. 44 (2008) 1126–1135.
[62] E. Diaz-Almeyda, P.E. Thome, M. El Hafidi, R. Iglesias-Prieto, Differential stability of photosynthetic membranes and fatty acid composition at elevated temperature in *Symbiodinium*, Coral Reefs 30 (2011) 217–225.
[63] S. Munné-Bosch, L. Alegre, The function of tocopherols and tocotrienols in plants, Crit. Rev. Plant Sci. 21 (2002) 31–57.
[64] D.J. Barshis, J.T. Ladner, T.A. Oliver, F.O. Seneca, N. Traylor-Knowles, S. R. Palumbi, Genomic basis for coral resilience to climate change, Proc. Natl. Acad. Sci. 110 (2013) 1387–1392.
[65] T.C. LaJeunesse, J.E. Parkinson, P.W. Gabrielson, H.J. Jeong, J.D. Reimer, C. R. Voolstra, S.R. Santos, Systematic revision of Symbiodiniaceae highlights the antiquity and diversity of coral endosymbionts, Curr. Biol. 28 (2018), 2570-2580. e2576.
[66] E.J. Howells, V.H. Beltran, N.W. Larsen, L.K. Bay, B.L. Willis, M.J.H. van Oppen, Coral thermal tolerance shaped by local adaptation of photosymbionts, Nat. Clim. Chang. 2 (2012) 116–120.
[67] L.J. Chakravarti, V.H. Beltran, M.J.H. van Oppen, Rapid thermal adaptation in photosymbionts of reef-building corals, Glob. Chang. Biol. 23 (2017) 4675–4688.
[68] A.F. Little, M.J.H. van Oppen, B.L. Willis, Flexibility in algal endosymbioses shapes growth in reef corals, Science 304 (2004) 1492–1494.
[69] A.C. Baker, Reef corals bleach to survive change, Nature 411 (2001) 765–766.
[70] S.B. Powles, Photoinhibition of photosynthesis induced by visible light, Annu. Rev. Plant Biol. 35 (1984) 15–44.
[71] B. Demmig-Adams, W.W. Adams, Photoprotection and other responses of plants to high light stress, Annu. Rev. Plant Biol. 43 (1992) 599–626.
[72] N. Murata, S. Takahashi, Y. Nishiyama, S.I. Allakhverdiev, Photoinhibition of photosystem II under environmental stress, Biochim. Biophys. Acta Bioenerg. 1767 (2007) 414–421.
[73] C.A. Oakley, G.W. Schmidt, B.M. Hopkinson, Thermal responses of *Symbiodinium* photosynthetic carbon assimilation, Coral Reefs 33 (2014) 501–512.
[74] K. Yonekura-Sakakibara, Y. Higashi, R. Nakabayashi, The origin and evolution of plant flavonoid metabolism, Front. Plant Sci. 10 - 2019 (2019).
[75] P. da Fonseca-Pereira, D.M. Daloso, J. Gago, F.M. de Oliveira Silva, J.A. Condori-Apfata, I. Florez-Sarasa, T. Tohge, J.-P. Reichheld, A. Nunes-Nesi, A.R. Fernie, W. L. Araújo, The mitochondrial thioredoxin system contributes to the metabolic

responses under drought episodes in Arabidopsis, Plant Cell Physiol. 60 (2018) 213–229.
[76] K. Apel, H. Hirt, Reactive oxygen species: metabolism, oxidative stress, and signal transduction, Annu. Rev. Plant Biol. 55 (2004) 373–399.
[77] D.A. Los, N. Murata, Membrane fluidity and its roles in the perception of environmental signals, Biochim. Biophys. Acta Biomembr. 1666 (2004) 142–157.
[78] V. Chinnusamy, J. Zhu, J.-K. Zhu, Cold stress regulation of gene expression in plants, Trends Plant Sci. 12 (2007) 444–451.
[79] S.G. Palusa, G.S. Ali, A.S.N. Reddy, Alternative splicing of pre-mRNAs of Arabidopsis serine/arginine-rich proteins: regulation by hormones and stresses, Plant J. 49 (2007) 1091–1107.
[80] J. Zhu, C.-H. Dong, J.-K. Zhu, Interplay between cold-responsive gene regulation, metabolism and RNA processing during plant cold acclimation, Curr. Opin. Plant Biol. 10 (2007) 290–295.
[81] H. Shin, S.-J. Hong, C. Yoo, M.-A. Han, H. Lee, H.-K. Choi, S. Cho, C.-G. Lee, B.-K. Cho, Genome-wide transcriptome analysis revealed organelle specific responses to temperature variations in algae, Sci. Rep. 6 (2016) 37770.
[82] M.-H. Liang, J.-G. Jiang, Advancing oleaginous microorganisms to produce lipid via metabolic engineering technology, Prog. Lipid Res. 52 (2013) 395–408.
[83] C. Liu, Y. Zhang, L. Huang, X. Yu, Y. Luo, L. Jiang, Y. Sun, S. Liu, H. Huang, Differences in fatty acids and lipids of massive and branching reef-building corals and response to environmental changes, Front. Mar. Sci. 9 (2022).
[84] S. Jandang, V. Viyakarn, Y. Yoshioka, C. Shinzato, S. Chavanich, The seasonal investigation of Symbiodiniaceae in broadcast spawning, *Aropora humilis* and brooding, *Pocillopora* cf. d*amicornis* corals, PeerJ 10 (2022).
[85] J. Helgoe, S.K. Davy, V.M. Weis, M. Rodriguez-Lanetty, Triggers, cascades, and endpoints: connecting the dots of coral bleaching mechanisms, Biol. Rev. 99 (2024) 715–752.
[86] L.A. Morris, C.R. Voolstra, K.M. Quigley, D.G. Bourne, L.K. Bay, Nutrient availability and metabolism affect the stability of coral–Symbiodiniaceae symbioses, Trends Microbiol. 27 (2019) 678–689.
[87] S.E. McIlroy, C.P. terHorst, M. Teece, M.A. Coffroth, Nutrient dynamics in coral symbiosis depend on both the relative and absolute abundance of Symbiodiniaceae species, Microbiome 10 (2022) 192.
[88] G. Cui, Y.J. Liew, Y. Li, N. Kharbatia, N.I. Zahran, A.-H. Emwas, V.M. Eguiluz, M. Aranda, Host-dependent nitrogen recycling as a mechanism of symbiont control in *Aiptasia*, PLoS Genet. 15 (2019) e1008189.
[89] G. Cui, Y.J. Liew, M.K. Konciute, Y. Zhan, S.-H. Hung, J. Thistle, L. Gastoldi, S. Schmidt-Roach, J. Dekker, M. Aranda, Nutritional control regulates symbiont proliferation and life history in coral-dinoflagellate symbiosis, BMC Biol. 20 (2022) 103.
[90] T. Krueger, N. Horwitz, J. Bodin, M.E. Giovani, S. Escrig, M. Fine, A. Meibom, Intracellular competition for nitrogen controls dinoflagellate population density in corals, Proc. Biol. Sci. 287 (2020) 20200049.
[91] S. Lin, L. Yu, H. Zhang, Transcriptomic responses to thermal stress and varied phosphorus conditions in *Fugacium kawagutii*, Microorganisms 7 (2019) 96.